Smart Structures and Systems, Vol. 11, No. 2 (2013) 185-197
DOI: http://dx.doi.org/10.12989/sss.2013.11.2.185

Simultaneous active strain and ultrasonic measurement using fiber acoustic wave piezoelectric transducers

J.R. Lee[1], C.Y. Park[2] and C.W. Kong[*3]

[1]*Department of Aerospace Engineering and LANL-CBNU Engineering Institute Korea, Chonbuk National University, Jeonju, South Korea*
[2]*Aeronautical Technology Directorate, Agency for Defense Development, Daejeon 305-600, South Korea*
[3]*Structures and Materials Department, Korea Aerospace Research Institute, Daejeon, South Korea*

(Received January 10, 2011, Revised October 7, 2012, Accepted October 27, 2012)

Abstract. We developed a simultaneous strain measurement and damage detection technique using a pair of surface-mounted piezoelectric transducers and a fiber connecting them. This is a novel sensor configuration of the fiber acoustic wave (FAW) piezoelectric transducer. In this study, lead-zirconate-titanate (PZT) transducers are installed conventionally on a plate's surface, which is a technique used in many structural health monitoring studies. However, our PZTs are also connected with an optical fiber. A FAW and Lamb wave are simultaneously guided in the optical fiber and the structure, respectively. The dependency of the time-of-flight of the FAW on the applied strain is quantified for strain sensing. In our experimental results, the FAW exhibited excellent linear behavior and no hysteresis with respect to the change in strain. On the other hand, the well-known damage detection function of the surface-mounted PZT transducers was still available by monitoring the waveform change in the conventional Lamb wave ultrasonic path.

Keywords: fiber acoustic wave; lamb wave; strain measurement; ultrasonic measurement; structural health monitoring

1. Introduction

In many studies, ultrasonic waves have been used in systems and structures to detect damage and evaluate safety. Rose (2004) indicated that ultrasonic waves are highly related to physical and environmental changes of the structure. However, conventional ultrasonic inspection of large structures is very time-consuming because the transducer needs to scan over each point of the structure to be tested. Hence, the use of ultrasonic guided waves is potentially a very attractive solution to this problem since they can be excited at one point of the structure and propagate over considerable distances. (Rose 2004, Zhao and Rose 2003, Alleyne and Cawley 1997) indicated that the ultrasonic guided waves have the potential to detect many types of structural damage and manufacturing defects that are not easily and efficiently detected by other means. (Giurgiutiu *et al*. 2002, Ihn and Chang 2004, Flynn *et al*. 2009, Kessler *et al*. 2002) have suggested that with advent of hardware technology that allows the integration of sensors and actuators into the structure and the development of methodology to perform damage detection, localization, evaluation, and

*Corresponding author, E-mail: kcw@kari.re.kr

visualization; structural health monitoring (SHM) based on built-in piezoelectric elements has become an important approach that is distinct from nondestructive piezoelectric ultrasonic evaluation. In this study, we used the concept of built-in piezoelectric transducers and the pitch-catch of structure-guided ultrasonic waves for damage detection. We also used a fiber waveguide for the pitch-catch of fiber-guided ultrasonic waves for strain measurement. The fiber-guided first-order longitudinal mode wave (L01), known as the fiber acoustic wave (FAW), can travel long distances with low attenuation. The small diameter of fibers such as optical and metal fibers also implies excellent probing and embedding capabilities. (Lee and Tsuda 2006, Neill *et al*. 2007, Chia *et al*. 2009) have emphasized that the strong directivity, high spatial resolution, and good cost-to-performance ratio makes the FAW piezoelectric transducer a valuable tool for SHM.

In many SHM studies, multifunctional sensing techniques for multi-physical quantities have been tried using fiber optic smart materials, which is another important SHM approach. Multifunctional sensing technology can improve the effectiveness of the SHM system only if each function can work without cross-talk with the other functions (e.g., simultaneous strain and passive acoustic emission monitoring using an extrinsic fiber Fabry-Perot interferometer (Bang *et al*. 2003) and fiber Bragg gratings (Koh *et al*. 2005), and strain and active ultrasonic sensing using fiber Bragg gratings (Betz *et al*. 2003). Even if one sensor was used to measure the dual physical quantities in the references listed above, two fiber optic sensor systems were required. Most other studies (Rajan *et al*. 2010, Alahbabi *et al*. 2004, Valdivielso *et al*. 2002, Mondal *et al*. 2009, Park *et al*. 2010, Caucheteur *et al*. 2004, Mahar *et al*. 2008, Zheng and Zhang 2005, Frazao *et al*. 2005) have examined simultaneous measurements of pressure, strain, and temperature.

To the authors' knowledge, studies on simultaneous measurement using piezoelectric transducers instead of fiber optic sensors have not yet been reported in the literature. (Kim *et al*. 2001, Vipperman 2001) have conducted the study on dual functionality of integrated piezoelectric sensors and actuators that are primarily focused on simultaneous damage detection and vibration control.

The main focus of this study concerns simultaneous strain and ultrasonic measurement based on built-in piezoelectric sensoriactuation. We demonstrate simultaneous strain measurement and pitch-catch damage detection by capturing a FAW guided in an optical fiber for strain measurement, and Lamb waves guided in an Al alloy plate, in a single time domain signal. The optical fiber is a simple optical fiber without a sensing element such as a fiber Bragg grating or an intrinsic Fabry-Perot interferometer, which is not connected with any optical sensing system.

2. Configuration of fiber acoustic wave piezoelectric transducers for simultaneous strain and ultrasonic measurement

2.1 Experimental setup

The experimental setup for the FAW piezoelectric transducers is shown in Fig. 1. Piezoelectric C-6 (Fuji ceramics) material of the Pb(Zr.Ti)O3 lead-zirconate-titanate (PZT) class was configured with a wrap-around electrode to collect the electrical leads on the top surface of the PZT. The longitudinal frequency constant (N_{31}) and the length (l) of the bar-shape PZT governs the resonance frequency (f_r) of the longitudinal motion:

$$N_{31} = f_r l \tag{1}$$

where N_{31} is 1420 m·Hz. Since the dimensions of the bar-shape bare PZT were 7 mm × 1 mm × 0.5 mm (l = 7 mm), the theoretical resonance frequency was 202 kHz for longitudinal vibration. Alternatively, cylindrical piezoelectric transducers (Taotao and Zhifei 2011, Wang *et al*. 2011) can be also used to make a FAW piezoelectric transducer depending on applications.

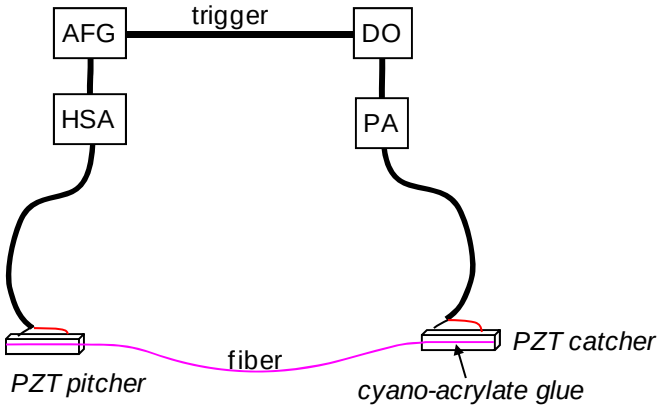

Fig. 1 Experimental setup for fiber acoustic wave PZT transducers (AFG: arbitrary function generator, HSA: high speed amplifier, PA: preamplifier, DO: digital oscilloscope, PZT: lead-zirconate-titanate)

The PZT transducers were connected by a fiber. For the fiber, a 135 μm polyimide-coated silica optical fiber was bonded on one surface of the PZT using cyano-acrylate adhesive. The excitation signal to the PZT ultrasonic actuator was a windowed 5-cycle sine tone-burst with a peak-to-peak voltage of 100 V_{pp} and a 100 ms burst period. Hamming window was used for narrowband ultrasound generation without side lobes. The signal received by the PZT ultrasonic receiver was amplified by a preamplifier. The signal was acquired with the options of 50 Ω impedance and a running average of 512 signals in a digital oscilloscope. The setup worked in this sequence: arbitrary function generator, high-speed amplifier, actuator, ultrasonic waves, receiver, preamplifier, and digital oscilloscope.

(Lee and Tsuda 2006) have described that an optical fiber as an ultrasonic waveguide, can be considered as a solid cylinder with layers. Hence, the longitudinal, flexural, and torsional modes exist theoretically. However, since the torsional mode cannot be guided in the optical fiber without intentional excitation control, only the longitudinal and flexural modes were considered. The theoretical group velocity dispersion curves for the 135 μm polyimide-coated optical fiber are shown in Fig. 2. The curves were calculated under the assumption that the elastic modulus is 73 GPa (http://accuratus.com/fused.html) for a fused silica fiber core with a diameter of 125 μm, and 2.7 GPa (Agag et al. 2001) for the 5 μm-thick polyimide coating. The theoretical group velocity of the FAW mode (L01) was almost constant at 5.14 km/s up to 2 MHz due to its small diameter.

2.2 Transducer configuration

Fig. 3(a) shows the typical pitch-catch configuration of PZTs for transmission of the Lamb

wave. One of the PZTs was used as an ultrasonic transmitter, while the other was used as an ultrasonic receiver. The Lamb wave was generated and propagated in a plate and was sensed by the ultrasonic receiver. Damage detection in the plate as a waveguide is possible by checking waveform parameter changes such as time-of-flight, amplitude, mode conversion, central frequency and frequency bandwidth. In contrast, Fig. 3(b) shows the same configuration but with an optical fiber installed as an additional waveguide parallel to the structure waveguide for the simultaneous pitch-catch of both FAW and Lamb wave by single ultrasonic transmission. Regarding the installation process, the lower surfaces of the two PZTs were first bonded onto the structure in the conventional configuration of surface-mounted PZTs. Then, the optical fiber was bonded to one of the PZTs. After the curing of the adhesive, the optical fiber was bonded to the other PZT with finger tension. The extra fiber length at both sides was cut because the extra fiber existence generates another reflective wave.

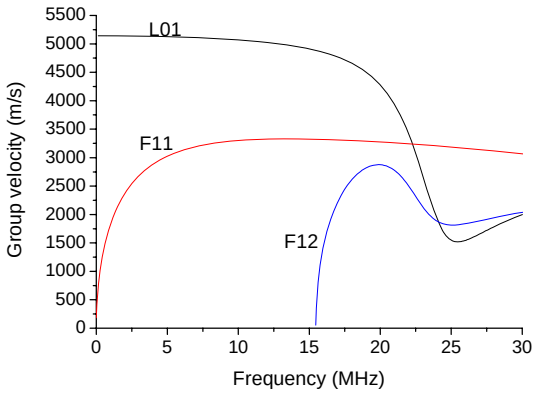

Fig. 2 Theoretical group velocity dispersion curves for the 135 μm polyimide-coated optical fiber (L01: first-order longitudinal mode, F11: first-order flexural mode, F12: second-order flexural mode)

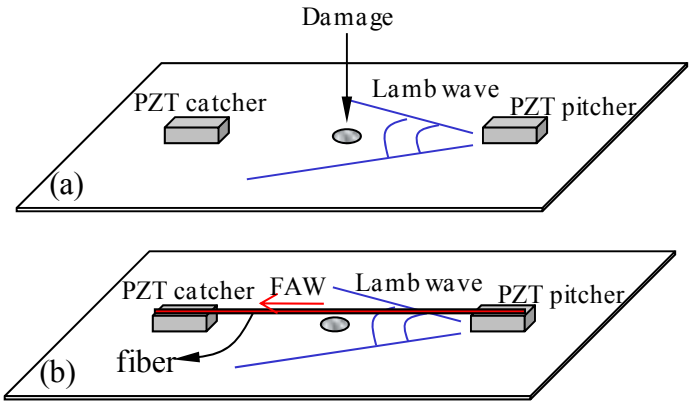

Fig. 3 (a) Lamb wave pitch-catch using a pair of surface-mounted PZTs, and (b) simultaneous pitch-catch of fiber acoustic wave and Lamb wave (FAW: fiber acoustic wave)

Consequently, the lower surfaces of the PZTs transmit and receive the Lamb wave while the surfaces bonded with the optical fiber transmitted and received the FAW. This configuration can be easily expanded for multi-area sensing using the configurations for FAW transducer trains shown in Fig. 4 and one centered PZT, and surrounding PZTs at various distances. The FAW transducer trains shown in Fig. 4 were used in the strain measurement test using the FAW. In this configuration, the pitcher PZT was installed on a fixed mount, and the catcher PZTs were surmounted on micro-translators capable of applying strain to the optical fibers. The lengths of the optical fibers were 250 mm, and the fixed mount and the micro-translators were fixed on an optical breadboard.

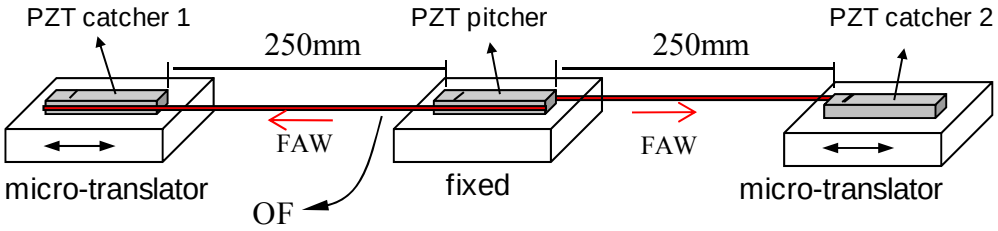

Fig. 4 Experimental setup for strain measurements using fiber acoustic waves (OF: 135 μm polyimide-coated optical fiber)

2.3 Fiber installation on the PZTs

The optical fiber was installed on the upper or side surface of the PZT, as shown in Fig. 5(a), to check if each surface of the PZT is available for the fiber installation because one PZT might have many fiber legs for sensor network construction. At this point, a combination of PZT pitcher and PZT catcher 1 from the setup shown in Fig. 4 was tested. Fig. 5(b) shows the waveforms detected successfully for the upper or side surface installations of the optical fiber at different excitation frequencies. The first-order flexural wave (F11) was negligible because it was very slow and dispersive as plotted in Fig. 2. Therefore, only the first-order longitudinal wave (L01) could be guided in the optical fiber and thus it was easily identified. The first wave packet corresponded to the direct FAW and traveled 250 mm from the pitcher PZT edge to the catcher PZT edge. The second wave packet was the first echo FAW, and traveled 750 mm, with the ultrasonic path of pitcher PZT edge/catcher PZT edge/pitcher PZT edge/catcher PZT edge. The small magnitude noisy waves between the direct wave and the first echo wave were caused by the reflection inside the fixed mount and the translator under the PZTs. In other words, the noisy waves are not related to simultaneous pitch-catch configuration of fiber acoustic wave and Lamb wave in Fig. 3(b). Therefore, these unwanted waves are not observed in the simultaneous measurement configuration with PZTs to be installed on a plate structure in Section 4. The time-of-flight of the direct FAW was 48.88 μs (48.66 μs), and the first echo FAW was three times the time-of-flight of the direct FAW, about 145.62 μs (145.02 μs) at 350 kHz (200 kHz) excitation. Therefore, the group velocities were measured at 5.13 km/s at 200 kHz and 5.12 km/s at 350 kHz, which are in good agreement with the theory described in Section 2.1.

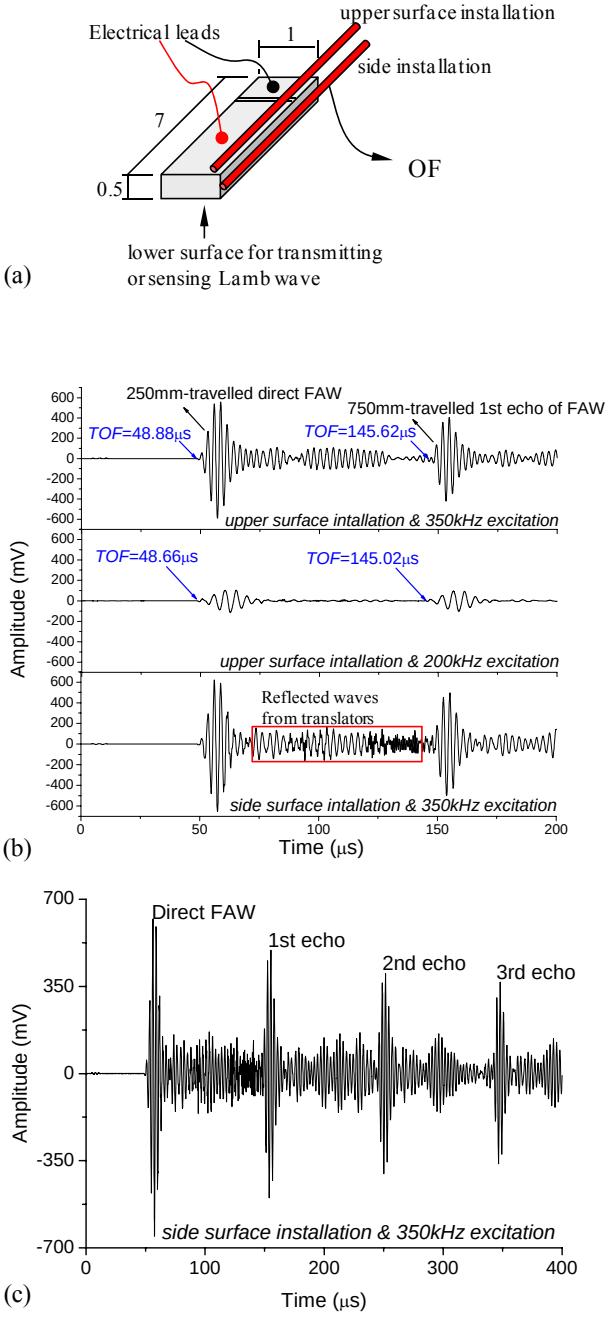

Fig. 5 (a) Optical fiber installation on the upper or side surface of the PZT transducer, (b) the direct and first echo fiber acoustic waves generated and detected in the 135 μm polyimide-coated optical fiber with different surface installations and frequencies, and (c) higher-order echo waves

3. Strain measurement by pitch-catch of the fiber acoustic wave

Using the side installation of the optical fiber on the PZTs, an experiment was conducted to analyze the relation between the FAW and the applied strain. As shown in Fig. 6, the strain applied by the micro-translator gave rise to a change in the waveform of the FAW traveling in the optical fiber waveguide by comparing the direct waves or the first echo waves before and after the strain effect. The variation in time-of-flight of the FAW is the major indication used to measure the strain applied to the host structure.

The direct and first echo detection of the FAW was analyzed at a 350 kHz excitation frequency. The direct wave traveled 250 mm while the first echo wave covered three times the distance (750 mm) in the fiber waveguide before being sensed. A 0.8% increase in strain decreased the time-of-flight of the direct wave by 1.16 μs, as shown in Fig. 6(b). A similar effect was induced in the first echo wave as shown in Fig. 6(c), where a 0.8% increase in strain caused a 3.46 μs decrease in time-of-flight. The variation in time-of-flight of the first echo wave was more significant and sensitive than that of the direct wave because the traveling distance was three times as long. Although a higher-order echo wave can be used for greater sensitivity, the first echo wave can be captured conveniently in a single time frame along with the Lamb wave used for damage detection without reduction in the time resolution. Therefore, the strain measurement using the first echo was chosen for this analysis. We note that the higher-order echo waves are still useful to measure strain with a higher sensitivity because even if the traveling distance is greatly increased due to repetition of echo, wave amplitude sufficient to detect change in wave time-of-flight is provided due to the low dispersion characteristics of the fiber waveguide. For example, Fig. 5(c) shows the fourth echo wave travelled 1,750 mm. In addition, an extremely long and cost-effective extensometer can be designed with the same configuration due to the long propagation capability of FAW.

As shown in Fig. 6, the first echo wave and direct wave exhibited sensitivities of 0.42 ns/με and 0.141 ns/με, respectively, and there was no hysteresis between loading and unloading. In addition, a polyimide-coated small diameter optical fiber with a total diameter of 50 μm (silica fiber diameter = 40 μm) was tested and compared to the 135 μm polyimide-coated optical fiber. The first echo wave in this waveguide exhibited a sensitivity of 0.5 ns/με, which was slightly higher than the sensitivity in the 135 μm polyimide-coated optical fiber. The 50-μm polyimide-coated optical fiber showed a low resistance to tensile strain and snapped at about 5,000 με, whereas a 135 μm polyimide-coated optical fiber sustained the strain without failure up to the test limit of 20,000 με. The small diameter optical fiber provided easy finger tension installation and a small pre-tension load to the PZTs, while the maximum measurable tensile strain was limited.

Regarding the measurement range, the tensile strain can be measured until the fiber snaps, but maximum compressive strain is dependent on the pre-tension applied to the fiber when it is installed. This is why Fig. 7 could not include lower compression region anymore which showed nonlinear behavior with respect to further compressive strain because of fiber buckling. Therefore, strain measurement and damage detection using this polyimide-coated optical fibers is limited to structural parts susceptible to tensile loading; for example, the lower surfaces of a bridge and an aircraft wing. Even if a pre-tension greater than finger tension could be applied to extend the compressive strain measurement range, we note that pre-tension could act as a considerable loading to the PZTs depending on the type of fiber. A higher pre-tension applicable fiber, e.g. a polymer fiber can be selected to obtain larger compressive strain measurement range but the

attenuation per distance and time-of-flight of FAW to be increased and the tensile strain measurement range to be reduced should be considered.

Finally, as shown in Fig. 8, the configuration of the FAW transducer trains allowed a multi-area strain measurement. A strain measurement in the range of -4,000 to 20,000 με was successfully demonstrated for the two gage lengths of the pitcher PZT-catcher PZT1 and the pitcher PZT-catcher PZT2.

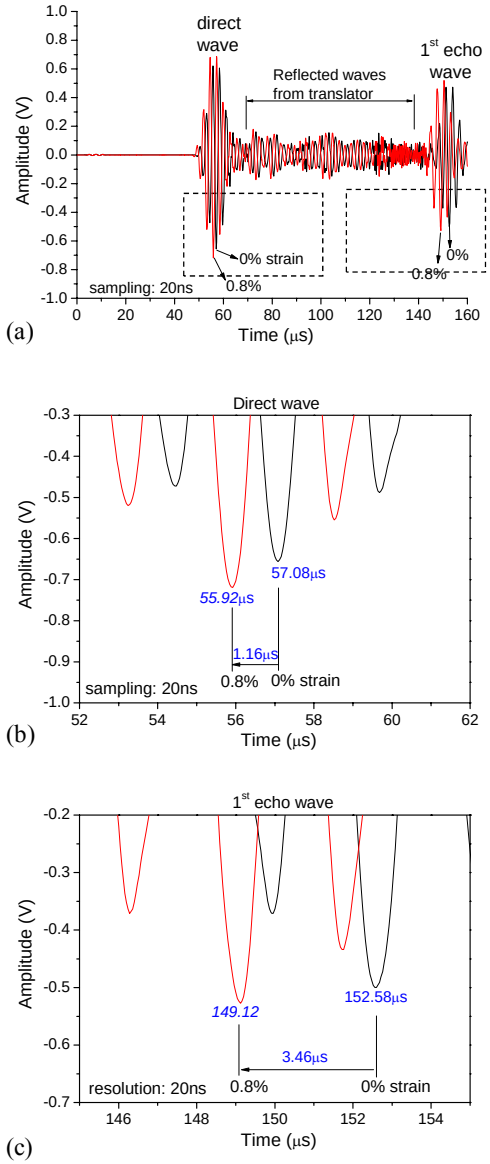

Fig. 6 (a) Fiber acoustic wave response with respect to a tensile strain of 0.8%, (b) strain-induced variation in time-of-flight of (b) the direct, and (c) first echo fiber acoustic wave.

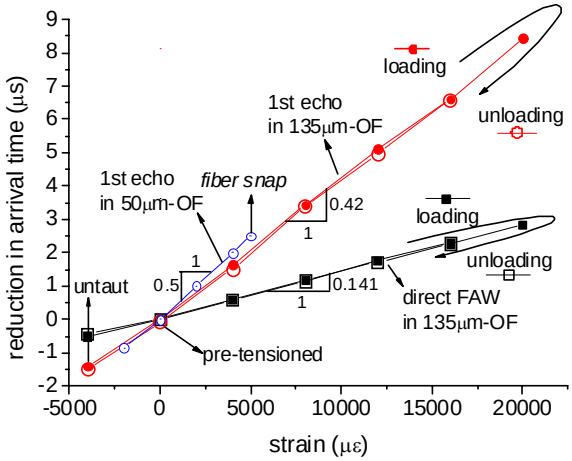

Fig. 7 Strain versus time-of-flight reduction of the direct and first echo fiber acoustic waves guided in the 135 μm and 50 μm polyimide-coated optical fibers

4. Damage detection by a lamb wave simultaneously generated with a fiber acoustic wave

Strain measurement using a FAW was described in Section 3. In this section, well-established damage detection technique using a Lamb wave is described in consideration of the simultaneously generated FAW. A pair of PZTs was bonded to an Al alloy plate with dimensions of 700 mm × 700 mm × 1 mm. The PZTs were separated by a distance of 237 mm and the excitation frequency was set to 330 kHz. Fig. 9(a) shows the transmission and detection of the Lamb wave guided in the plate with zeroth-order symmetrical (S0) and asymmetrical (A0) modes. A 135 μm polyimide-coated optical fiber was installed between two PZTs for a before-and-after comparison of the optical fiber installation. As shown in Fig. 9(b), the S0 mode wave overlapped with the direct FAW because the group velocities were similar (5.25 km/s for the S0 mode and 5.12 km/s for the FAW), and both waves traveled the same distance. In this case, the S0 mode wave mixed with the FAW cannot be easily used for damage detection without a special signal processing algorithm. On the other hand, the A0 mode was independent of both the direct FAW and the first echo FAW for strain measurement due to its low group velocity of 2.48 km/s. Therefore, the A0 mode was used for damage detection using the Lamb wave. As we controlled here to obtain the two separated waves in a single time signal, a guided wave mode and an order-of-echo wave can be selected by controlling parameters such as the measurement distance determining time-of-flights of echo waves and the fiber material and dimensions including the coating determining group velocity of FAW.

The Al alloy specimen was scratched with a rotating saw to create crack-like damage in the middle of the two PZTs, as shown in Fig. 10(a). Waveform acquisition was conducted again for the damaged specimen and the resulting waveforms before and after the damage are compared in Fig. 10(b). The significant decrease (3.36 dB loss) in wave magnitude of the A0 mode indicates the damage detection. Even if the S0 mode was mixed with the FAW, the S0 mode also provided

another damage indication in the form of a mode-converted wave. As presented in the wavelet coefficient scalograms in Fig. 10(c) and (d), the damage indication was also clear in frequency domain.

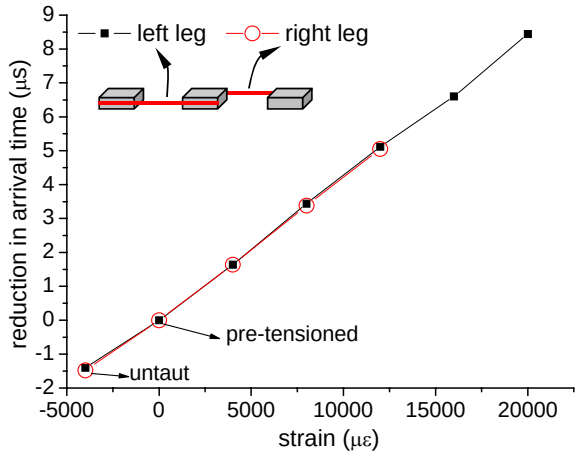

Fig. 8 Demonstration of multi-area strain measurement by fiber acoustic wave PZT transducer trains

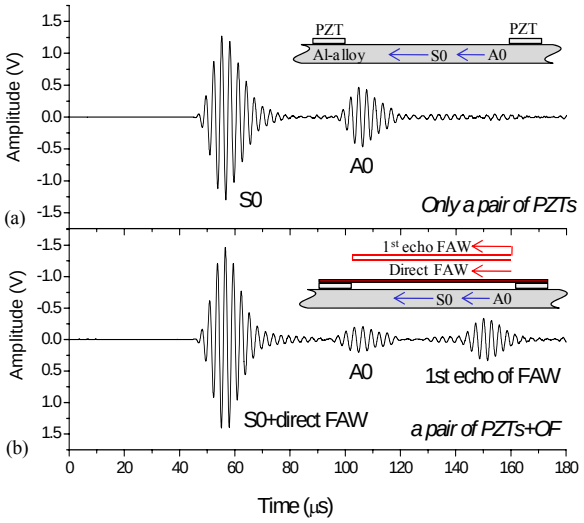

Fig. 9 (a) Detection of only Lamb wave without the optical fiber, and (b) simultaneous measurement of FAW and Lamb wave with the optical fiber in the 1 mm-thick Al alloy plate at 330 kHz excitation

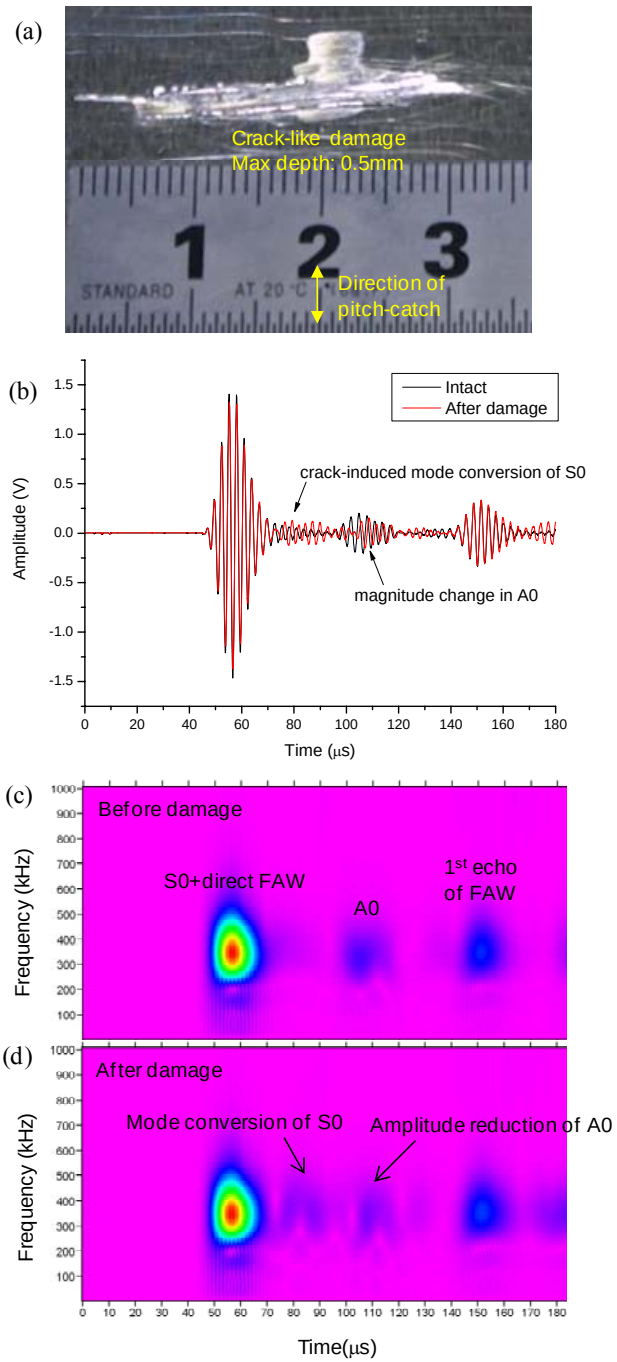

Fig. 10 (a) Crack-like damage generated on the surface of the Al-alloy plate, (b) waveform change indicating damage detection, and wavelet coefficient scalograms (c) before and (d) after the damage

Consequently, a Lamb wave and FAW were simultaneously generated and detected by adding the optical fiber into the configuration of the conventional surface-mounted PZTs. The A0 mode of the Lamb wave and the first echo wave of the FAW were arranged in a single time signal to perform simultaneous damage detection and strain measurement. The strain measurement was described in Section 3, and the damage detection was demonstrated in this section by detecting the surface crack.

5. Conclusions

A novel sensing configuration of a FAW PZT transducer was proposed. Our application was easily realized by installing a fiber onto surface-mounted PZTs in a configuration that is well-established for SHM. A Lamb wave and FAW were simultaneously generated by an excitation PZT and were propagated independently over an Al alloy plate and an optical fiber, respectively. The waves were then detected together by a sensing PZT in a single time frame. The new ultrasonic path made from the additional fiber waveguide between a pair of PZTs provided strain measurement capability by monitoring the variation in the time-of-flight of the FAW, which exhibited excellent linear behavior and no hysteresis with respect to the strain change. The damage detection function of the PZTs was available through the conventional Lamb wave ultrasonic path by monitoring the waveform change.

Acknowledgements

This research was supported by Leading Foreign Research Institute Recruitment Program through the National Research Foundation of Korea funded by the Ministry of Education, Science and Technology (2011-0030065). This research was also supported by the University Collaboration Enhancement Project of the Korea Aerospace Research Institute and by the research grant (UD120027JD) of the Agency for Defense Development of the Korean government.

References

Agag, T., Koga, T. and Takeichi, T. (2001), "Studies on thermal and mechanical properties of polyimide - clay nanocomposites", *Polymer*, **42**(8), 3399-3408.

Alahbabi, M.N., Cho, Y.T. and Newson, T.P. (2004), "Simultaneous distributed measurements of temperature and strain using spontaneous Raman and Brillouin scattering", *Proceedings of the EWOFS 2004,*Santander, Spain, June.

Alleyne, D.N. and Cawley, P. (1997), "Long range propagation of Lamb waves in chemical plant pipework", *Mater. Eval.,* **55**(4), 504-508.

Bang, H.J., Kim, D.H., Kang, H.K., Hong, C.S. and Kim, C.G. (2003), "Optical fiber sensor systems for simultaneous monitoring of strain and damage in smart composites", *Proceedings of the SPIE 5050,* San Diego, USA, March.

Betz, D.C., Thursby, G., Culshaw, B. and Staszewski, W.J. (2003), "Acousto ultrasonic sensing using fiber Bragg gratings", *Smart Mater. Struct.,* **12**(1), 122-128.

Caucheteur, C., Lhomme, F., Maakaroun, F., Chah, K., Blondel, M. and Megret, P. (2004), "Simultaneous strain and temperature sensor using superimposed tilted Bragg gratings", *Proceedings of the Symp. IEEE/LEOS Benelux Chapter*, Ghent, Belgium, Dec.

Chia, C.C., Lee, J.R. and Shin, H.J. (2009), "Hot target inspection using a welded fibre acoustic wave piezoelectric sensor and laser ultrasonic mirror scanner", *Meas. Sci. Technol.,* **20**(12), 127003.

Flynn, E.B., Swartz, A., Backman, D.E., Park, G. and Farrar, C.R. (2009), "Active-sensing Lamb wave propagation for damage identification in honeycomb aluminum panels", *J. Korean Society for Nondestructive Testing,* **29,** 269-282.

Frazao, O., Ramos, C.A., Pinto, N.M.P., Baptista, J.M. and Marques, A.T. (2005), "Simultaneous measurement of pressure and temperature using single mode optical fibres embedded in a hybrid composite laminated", *Comp. Sci. Technol.,* **65**(11-12), 1756-1760.

Giurgiutiu, V., Zagrai, A. and Bao, J.J. (2002), "Piezoelectric wafer embedded active sensors for aging aircraft structural health monitoring", *Struct. Health Monit.,* **1**(1), 41-61.

Ihn, J.B. and Chang, F.K. (2004), "Detection and monitoring of hidden fatigue crack growth using a built-in piezoelectric sensor/actuator network: II Validation using riveted joints and repair patches", *Smart Mater. Struct.,* **13**(3), 621-630.

Kessler, S.S., Spearing, S.M. and Soutis, C. (2002), "Damage detection in composite materials using Lamb wave methods", *Smart Mater. Struct.,* **11**(2), 269-278.

Kim, M.H., Pakr, G. and Inman, D.J. (2001), "Simultaneous control and monitoring of adaptive structures using smart sensors', *Proceedings of the IMAC-XIX: A Conference & Exposition on Structural Dynamics,* Kissimmee, Florida, USA, Feb.

Koh, J.I, Bang, H.J., Kim, C.G. and Hong, C.S. (2005), "Simultaneous measurement of strain and damage signal of composite structures using a fiber Bragg grating sensor", *Smart Mater. Struct.,* **14**(4), 658-663.

Lee, J.R. and Tsuda, H. (2006), "Investigation of a fiber wave piezoelectric transducer", *Meas. Sci. Technol.,* **17**(9), 2414-2420.

Mahar, S., Geng, J., Schultz, J., Minervini, J., Jiang, S., Titus, P., Takayasu, M., Gung, C.Y., Tian, W. and Arturo, C.P. (2008), "Real-time simultaneous temperature and strain measurements at cryogenic temperatures in an optical fiber", *Proceedings of the SPIE,* San Diego, USA, Aug.

Mondal, S.K., Mal, S., Tiwari, U., Sarkar, S., Mishra, V., Poddar, G.C., Mehla, N.S., Jain, S.C. and Kapur, P. (2009), "Simultaneous measurement of strain and temperature using partially etched single fiber Bragg grating sensor ", *Proceedings of the ICOP-200,* Chandigarh, India, Oct- Nov.

Neill, I.T, Oppenheim, I.J. and Greve, D.W. (2007), "A wire-guided transducer for acoustic emission sensing", *Proceedings of the SPIE 6529,* San Diego, March.

Park, S.O., Jang, B.W., Lee, Y.G., Kim, C.G. and Park, C.Y. (2010), "Simultaneous measurement of strain and temperature using a reverse index fiber Bragg grating sensor", *Meas. Sci. Technol*., **21**(3), 035703.1-8.

Rajan, G., Mileńko, K., Lesiak, P., Semenova, Y., Boczkowska, A., Ramakrishnan, M., Jędrzejewski, K., Domański, A., Woliński, T. and Farrell, G. (2010), "A hybrid fiber optic sensing system for simultaneous strain and temperature measurement and its applications", *Photonics Letters of Poland,* **2**(1), 46-48.

Rose, J.L. (2004), *Ultrasonic Waves in Solid Media,* Cambridge University Press, Cambridge.

Taotao Z. and Shi Zhifei S. (2011) "Exact solutions of the piezoelectric transducer under multi loads", *Smart Struct. Syst.*,**8**(4), 413-431.

Valdivielso, C.F., Matias, I.R. and Arregui, F.J. (2002), "Simultaneous measurement of strain and temperature using a fiber Bragg grating and a thermochromic material", *Sens. Act. A:Physical,* **101**(1-2), 107-116.

Vipperman, J.S. (2001),"Simultaneous qualitative health monitoring and adaptive piezoelectric sensoriactuation", *AIAA J*., **39**(9), 1822-1825.

H.M. Wang, Y.K. Wei and Z.X. Xu (2011), "Radial vibration behaviors of cylindrical composite piezoelectric transducers integrated with functionally graded elastic layer", *Struct. Eng. Mech.*, **38**(6), 753-766.

Zhao, X.L. and Rose, J.L. (2003), "Boundary element modeling for defect characterization potential in a wave guide", *Int. J. Solids Struct.,* **40**(11), 2645-2658.

Zheng, S. and Zhang, X. (2005), "Simultaneous measurement of pressure and temperature using a single fiber Bragg grating", *Proceedings of the Electromagnetics Research Symp.,* Hangzhou, China, Aug.